Characterisation of Electric Bicycles Performances.

Jan Cappelle, Philippe Lataire, Gaston Maggetto, Romain Meeusen, Farid Kempenaers

Abstract

The proposed paper reports on characterisation work performed in the scope of the E-tour project. This project has already been presented at EVS-18.

At the 'Vrije Universiteit Brussel' different EPACs (Electric Power Assisted Cycles) are put at the public's disposal for testing. To quantify the performances of these electrical bicycles we want to link the subjective experienced driving comfort to some measurable objective parameters. For this purpose we converted a treadmill into a test bench for two-wheelers. Extra effort has been made to achieve a good approximation of the road conditions. The front and rear wheel are both rolling on a flat treadmill, driven by an AC-drive. A crowbar can adjust the slope of the bench. The cyclist has been replaced by a controlled DC-drive that drives the pedals by means of an angular gearbox and a pulley. In order to prevent relative motion of the bicycle with reference to the belt, a chain with load-cell is connected between the bicycle and the treadmill. The force measured by the load-cell is the traction force that will be used to characterise the performance of the EPACs.

This paper starts with the results of an exploring road test, followed by the description of the construction of the test application. Another paragraph discusses the definition of the performance parameters: efficiency and assistance factor. Finally, we discuss the measurement results of the traction forces and the performance parameters of 3 different types of EPACs: A Merida GMB Euro-scoot, a Sachs Elo-bike and a yamaha PAS. © *Copyright 2002 EVS19*.

Keywords: bicycle, PAS(power assist system), vehicle performance, efficiency.

1. Road Test

1.1. Description of the Road Test

Before putting bicycles on the test bench, we performed a little road test to examine in what degree differences in bicycle efficiency can be felt by the cyclist. The road test gave us a first indication of the difference in efficiency we should be able to quantify with the test bench. It gave us also an idea of power and torque limits on the crankshaft under real conditions.

If the route, the pedalling speed and the transmission are kept constant and the air resistance is not changing too much, the traction used by the bicycle is considered to be the same and the power delivered by the cyclist will be a measure for efficiency.

The human power was measured by means of the heart rate of the subject. In order to know the relationship between those quantities the subject underwent a calibrating procedure on an electrically braked cycle ergo meter.

The test started at 80 Watts and each 3 minutes the resistance of the cycle ergo meter was raised by 30 Watts. An optimal cadence of 90 rpm is kept constant during the test.

Blood lactate and heart rate measurements were performed at the end of every 3-minute stage. These calibration results are given in figures 1 and 2.

The subject was a male student, (weight=88kg, length=1.92m, BMI=23.9) of moderate physical condition. Notice the almost linear relationship between heart rate and delivered power beneath the 180 bpm, this is the aerobic treshold of the subject (figure 1).
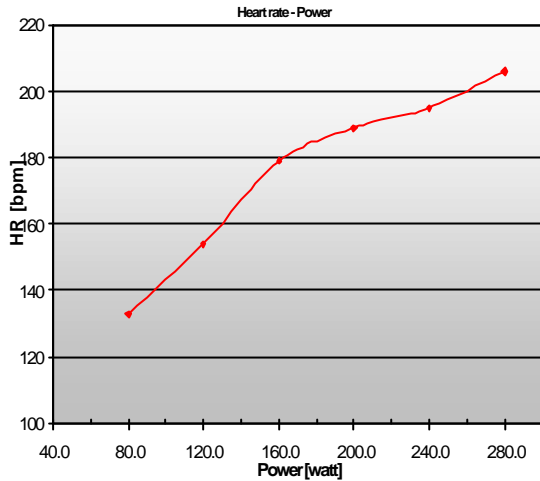
Figure 1: Heart rate vs. human power output.   Figure 2: Blood lactate vs. heart rate.
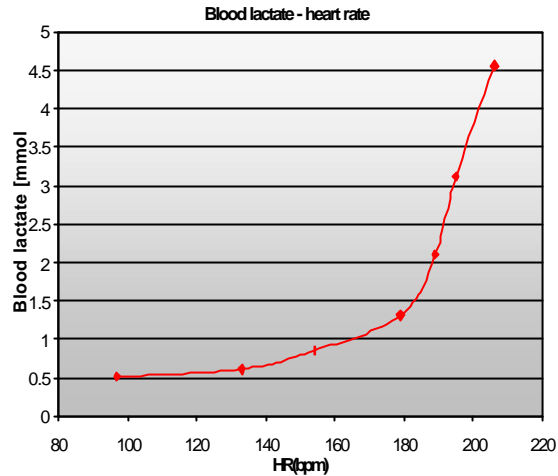
The chosen route was 400 m long without any noticeable slopes.
We did the tour with the electrical assisted GMB Euro-scoot L'avenir (Merida) and with a non-assisted mountain bike (MBK).

We performed 4 different cases:
1. Non-assisted Merida
2. Assisted Merida
3. Non-assisted Merida with uncomfortable position (low saddle)
4. MBK

Except for case 3, all cases were performed at different speeds: 10, 15, 20, 25 km/h. In order to compare series 1 and 4 with respect to the air resistance, the subject drove the MBK upright and hands free.

## 1.2. The Results

The results are given in figure 3
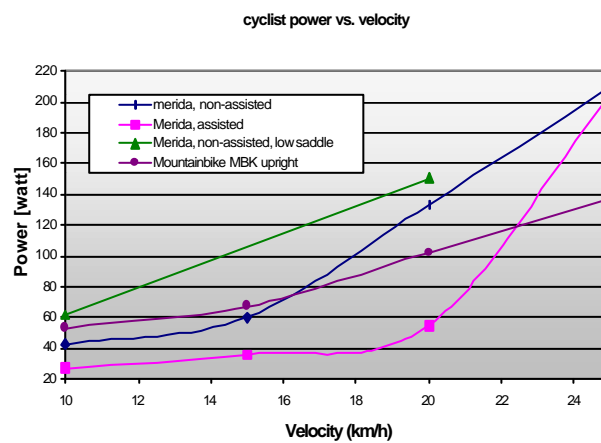
Figure 3: power output vs. velocity for 4 different road tests.

The graphs roughly show the squared relationship between air-resistance and velocity.
The following conclusions can be drawn from this road test:

- The electrical assistance of the Merida (3rd speed) diminishes from 100 % to 0% in the area from 20 to 25 km/h. This is further confirmed by the measurements on the test bench.
- Due to it's smaller weight, the mountain bike seems to be the most efficient bike for higher speeds. Notice the bad efficiency of the Merida above 20 km/h.
- The low saddle situation is added to show the importance of the cyclist's position. This factor is not included in the measurements on the test bench.
- The assistance of the Merida roughly seems to halve the needed human power in the range from 0 to 20km/h, which will be quantified by measurements on the test bench.

1.3. Operation Area

The road test gave us an idea of the power and torque limits brought to the pedals during cycling, When a person of 100 kg pushes the pedals with full mass and pulls to his steer to get 200N more, the peak torque on a crank of 17 cm will reach:

$$T = mgl = 120 * 9.81 * 0.17 \approx 200\,Nm \qquad (1)$$

Taking into account the pulsating character of the torque (figure 6), this peak torque results in a mean torque of 115 Nm. The maximum rotational speed was set to 160 rpm, a value that rarely will be reached under normal conditions. As experienced during the calibration test, the production of 300 W can be taken as upper limit for a person of common fitness.
In this way we get the marking out of the operation area of the DC-motor, used to replace the cyclist on the test bench (figure 4).
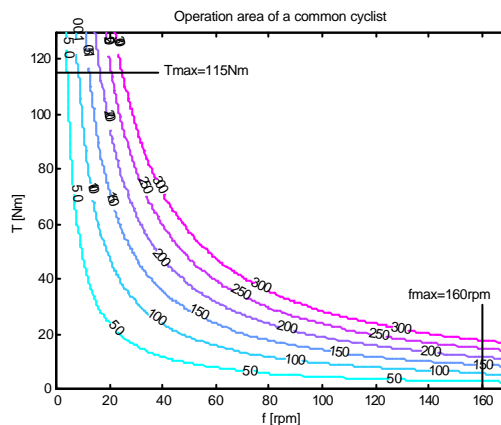

Figure 4: operation area of the (dummy) cyclist

2. Design of the Test Application

In order to quantify the performances of the electric two-wheeler, we need to *measure the force* that the bike develops *under real conditions*

1. to accelerate
2. to defeat slopes
3. to defeat air-resistance

as a function of *torque on the pedals, the gear and the velocity*.
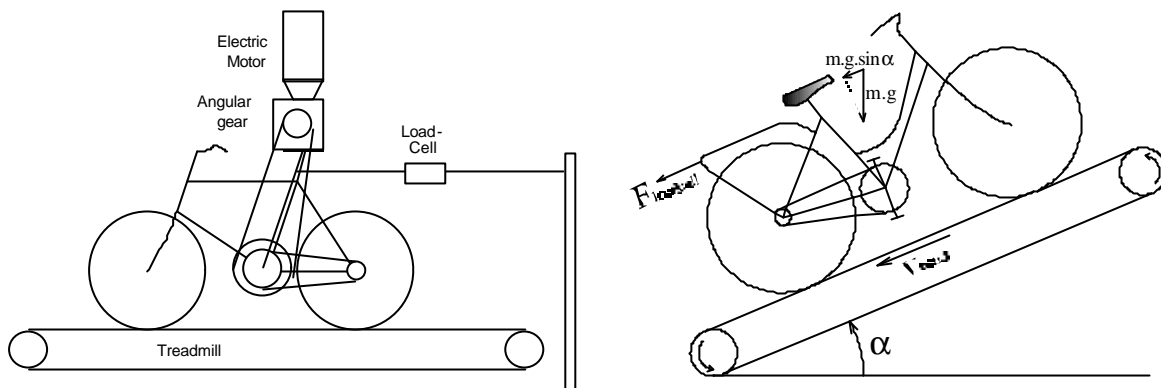
Figure 5: Construction of the test bench

2.1. Imitation of the Road Conditions

Most of the existing test apparatus fix the two-wheelers by some mechanism introducing extra reaction forces that are not present under real conditions. Also the removal of a wheel is undesirable. To prevent this, we wanted the bike to roll freely on a conveyor belt by its two wheels. Therefore, a runners treadmill is extended and adapted to the special operating conditions. The used conveyor belt has a width of 500 mm and a thickness of 2.8mm. It is composed of four layers of which the uppermost is a smooth adhesive PVC layer, imitating the road surface. The total length of the test installation is about 3 meters. The whole bench can be lifted to simulate slopes and to bring in some extra (exactly known) load when executing tests with higher torques. For safety reasons the whole test bench is enclosed. During tests a person outside the test safety cage is steering, to keep the bike upright.

2.2. Input Variables

2.2.1. Torque

As a first input to the bicycle we have the torque applied to the pedals. Therefore a dummy cyclist has been designed. This is a DC-motor with angular gearbox, mounted on the saddle rod. A pulley and a torque sensor (Lorenz MR-12, 500Nm, accuracy class 0.15) replace the pedals and their cranks. Transmission is performed by a V-belt. An optical encoder in the torque sensor delivers a TTL-signal from which the rotational speed of the pulley can be derived. By supplying the DC-motor by a controlled thyristor rectifier, we are able to impose either a constant or pulsating torque. Observing the torque delivered by a cyclist (figure 6), it's almost a sine wave with an offset of 115% of the amplitude. That's the torque time evolution we selected to work with.
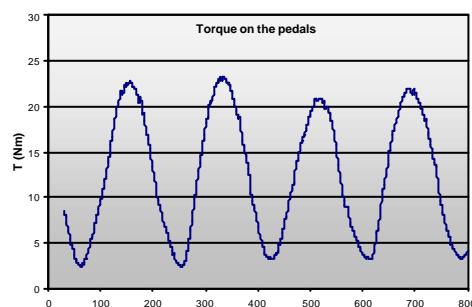

Figure 6: Torque on the pedals during cycling

2.2.2. Gear

For the bicycles tested on the bench, we measured the transmission rate Z between the linear speed of the wheels and the rotational speed of the pedals for every gear. (tables 1 2 and **3**)

$$Z = \frac{\Delta x}{\boldsymbol{a}_{rad}} = \lim_{\Delta t \to 0} \frac{\frac{\Delta x}{\Delta t}}{\frac{\boldsymbol{a}_{rad}}{\Delta t}} = \frac{v}{\boldsymbol{w}} \tag{2}$$

gear	Z
1	0,539
2	0,679
3	0,829
4	0,985

Table 1: Transmission rates of the GMB Euro-scoot, L'avenir (Merida)

gear	Z
1	0.532
2	0.654
3	0.792
4	0.968

Table 2 Transmission rates of the Yamaha PAS

gear	Z
1	0.506
2	0.674
3	0.897

Table 3 Transmission rates of the Sachs ELO-Bike

2.2.3. Speed

The speed of the bicycle wheels is determined by the conveyor belt speed. An induction motor, supplied by a frequency converter (ABB Sami GS) drives the belt, so speed can be adjusted. Comparison between speed measurements of a tachometer (mounted on an intermediary axis of this drive) and the TTL signal of the torque sensor on the crankshaft learns that no noticeable slip exists between the tyre and the conveyor belt.

2.3. Output Variable

To prevent relative motion of the bicycle with reference to the belt, a chain with load-cell is attached to the test model. The load-cell is a Sensy model 2712, 50 daN calibrated to reach its full-scale range for 15 daN (accuracy class 0.1). This showed to be useful for measuring at relative low traction forces and equally protects for peak forces when applying pulsating torques. For a better dynamic behaviour we introduced a spring (k=2916 N/m) between load-cell and bicycle.

2.4. Data Acquisition and Automate Control

2.4.1. Data acquisition

The data acquisition applied for the tests is a VXI system of HP combined with a Labview user interface.
The 4-20 mA current signal of the load-cell is converted by a resistance into a voltage signal and read by the digitiser (HP E1429B).
Combined with a multiplexer, the digitiser also interprets the torque signal of the torque sensor. The TTL-signal of the torque sensor is send through a low-pass filter and differential amplifier before being read by a time interval analyser (HP1740A).
A digital multimeter (HP E1411B) performed offset measurements of the torque and the traction force signals.

2.4.2. Automate control

The torque applied to the pedals, and speed of the conveyor belt can be adjusted by use of a VXI D/A converter (HP E1328A). The user interface is again a Labview program. So it becomes quite easy to apply different load conditions to the bicycle.

3. Discussion on the Measurement Method

3.1. Remarks on the Pulsating Input

For calculations of efficiency and assistance factor we'll reason on power flows. When applying a constant torque, the calculation of the average power delivered by the cyclist is easy:

$$P_c = \frac{1}{t_2 - t_1} \int_{t_1}^{t_2} T_c(t).w(t).dt = T_c.w \tag{3}$$

where ù is the rotational speed of the pedals, T_c the torque applied on the crank shaft and t_2-t_1 is the measuring time interval.

As described above we prefer to apply a torque consisting of a constant component and an alternating component. As shown in paragraph 2.2.1 formula (4) is a good approximation of the human torque:

$$T = \overline{T}\left(1 + 0.74 \sin\left(2\overline{w}t\right)\right) \tag{4}$$

with $\overline{w}$ the mean of the rotational speed of the pedals. This pulsating input results in a pulsating ω and v. Also the traction force can be pulsating. To average the traction force, as much as possible, we introduced a spring. The spring did a good job for most of the measurement points, but could not prevent heavier pulsation in following cases:

- Torques on bicycles delivering pulsating assistance caused by a fast sampling of the assistance determining parameters.
- Torques near Tmax.
- Pulsations near the resonance frequency of the mass-spring system.

Supposing all pulsations are the same, an extra term appears when calculating the power integral:

$$P_c = \overline{w}.\overline{T}_c + \frac{1}{2}(0.74)^2 \, \overline{w}.\overline{T}_c \cos(j) \tag{5}$$

where φ is the phase shift between T_c and ω. It seems no longer correct to average T_c and ω separately. So we need a simultaneous registration of the torque T and the angular speed ω signals, which was not available at the time of the tests. So T and ω were averaged separately.

But still, the average traction force as described below is a good parameter to evaluate the performance of the bicycles. For the calculation of efficiency and assistance (see § 3.3 and § 3.4) the influence of the phase delay will be negligible if speed delay approaches 90 degrees. In other cases, the influence has to be studied.

3.2. Traction Force

For every test object we'll make a 3D plot of the mean traction force $\overline{F}_t$ as a function of mean rotational speed $\overline{\omega}$ and the mean torque of the cyclist $\overline{T}_c$.

$$\overline{F}_t = f_1\left(\overline{w}, \overline{T}_c\right) \tag{6}$$

Depending on the type of bicycle (see § 3.6) we should record $\overline{F}_t$ for different gears. The traction force is the sum of the force measured by the load-cell and, in the event the bench is lifted, the needed force to keep the bike in balance (figure 5).

$$F_t = F_{loadcell} + mg \sin a \tag{7}$$

At the moment the described measurements were taken, the lifting of the bench wasn't used. The 3D plot of the traction force has been referred to as the *output plot*.

3.3. Efficiency

Due to the experienced low efficiency of the electric bike without assistance (see § 1.2), we are interested how much the complex mechanism for adding motor and cyclist torque influences the mechanical efficiency. The efficiency will be calculated as function of mean torque and speed in the so-called *efficiency plot*.

$$\boldsymbol{h} = f_2\left(\overline{\boldsymbol{w}}, \overline{T}_c\right) \tag{8}$$

Efficiency can be defined as power input divided by power output. Only if assistance is switched-off, η can be considered as the mechanical efficiency.

$$\boldsymbol{h} = \frac{P_t}{P_c} = \frac{\dfrac{1}{t_2 - t_1}\displaystyle\int_{t_1}^{t_2} F_t(t).v(t).dt}{\dfrac{1}{t_2 - t_1}\displaystyle\int_{t_1}^{t_2} T_c(t).\boldsymbol{w}(t).dt} = \frac{\overline{F}_t.\overline{v}}{\overline{T}_c.\overline{\boldsymbol{w}}} = \frac{\overline{F}_t}{\overline{T}_c}.Z \tag{9}$$

where P_t is the virtual power that under road conditions is at the cyclist's disposal. Notice that P_t is not consumed at the load-cell of the test application. It will partly disappear in friction of the conveyor belt and the rollers and partly be used for driving the belt drive system. If this power gets too high, a brake chopper has to be installed in the drive. The last two expressions of equation (9) are only valid for constant torques. In case of pulsating torques, the integration should be executed (see § 3.1).

3.4. Cyclist's Force

By plotting the total traction force $\overline{F}_t$ as a function of the cyclist's torque $\overline{T}_c$. We compare torques and forces. It is more interesting to refer everything to the same level: either forces at the loadcell, or torques at the pedals.

The power available for traction originates from two sources: power coming from the assistance motor and power coming from the cyclist.

Beside P_t and P_c (see 3.2), we define P_{as} as the useful power of the assistance motor that is available for traction. The power equation becomes:

$$P_t = \boldsymbol{h}P_c + P_{as} \tag{10}$$

Notice that P_{as} cannot be directly measured, but has to be derived from comparison between assisted and non-assisted situations for the same cyclist's torque and conveyor belt speed.

$$P_{as} = P_{t-A} - P_{t-NA} \tag{11}$$

Working out the power equation results in a division of the total force $\overline{F}_t$ in a cyclist's force $\overline{F}_c$ and an assistance force $\overline{F}_{as}$:

$$\frac{1}{t_2 - t_1}\int_{t_1}^{t_2} F_t(t).v(t).dt = \boldsymbol{h}\frac{1}{t_2 - t_1}\int_{t_1}^{t_2} T_c(t).\boldsymbol{w}(t).dt + \frac{1}{t_2 - t_1}\int_{t_1}^{t_2} F_{as}(t).v(t).dt \tag{12}$$

For steady-state situations and constant torques applied to the pedals, this reduces to:

$$\overline{F}_t = \frac{\boldsymbol{h}\overline{T}_c}{Z} + \overline{F}_{as} = \overline{F}_c + \overline{F}_{as} \tag{13}$$

The term $\dfrac{\boldsymbol{h}\overline{T}_c}{Z}$ is the contribution of the cyclist to the total traction force, or shortly the cyclist's force $\overline{F}_c$.

The real force delivered by the cyclist will be bigger, because of the mechanical transmission. This real cyclist's force can be easily derived from the measurements by using equation (13):

$$\frac{\overline{F}_c}{h} = \frac{\overline{T}_c}{Z} \tag{14}$$

For every tested bicycle, we determined a 3D *performance plot*: the total traction force $\overline{F}_t$ versus the real cyclist's force $\dfrac{\overline{F}_c}{h}$ and the linear speed v. Slices of these performance plots are given below.

3.5. Assistance Factor

Another interesting topic is the evolution of the part of assistance in the total power output as a function of torque and speed.

$$\boldsymbol{x} = f_3\!\left(\overline{w}, \overline{T}_c\right) \tag{15}$$

The assistance factor ξ will be defined as the power output coming from the assistance motor divided by the total power output:

$$\boldsymbol{x} = \frac{P_{as}}{P_t} \frac{\dfrac{1}{t_2 - t_1}\displaystyle\int_{t_1}^{t_2} F_{as}(t).v(t).dt}{\dfrac{1}{t_2 - t_1}\displaystyle\int_{t_1}^{t_2} F_t(t).v(t).dt} = \frac{\overline{F}_{as}}{\overline{F}_t} = 1 - \frac{\overline{F}_c}{\overline{F}_t} \tag{16}$$

As for efficiency, the last expressions are only true under certain conditions.

$\xi=0$ if $\overline{F}_c = \overline{F}_t$, thus if all traction originates from the cyclist.

$\xi=1$ if $\overline{F}_c = 0$, thus if all traction originates from the assistance motor.

3.6. Influence of Gearbox

The role of the gearbox in the performance parameters that are described above, depends on the type of the assistance.

3.6.1. Type 1: assistance at the crankshaft.

For two-wheelers of type 1, the control system determines the assistance by measurements at the crankshaft. The assistance motor is mostly situated near the chainwheel.
So if ω and T_c are the same, but we shift from one to another gear, the torque coming from the assistance motor $\overline{T}_{as}$ will not change. At the level of the crankshaft, assistance is totally defined. By measuring $\overline{F}_t$ in one gear i, the traction force in gear j can be derived by:

$$\overline{F}_{tj} = \frac{h}{Z_j}\left(\overline{T}_{as} + \overline{T}_c\right) = \frac{Z_i}{Z_j}\overline{F}_{ti} \tag{17}$$

Possible spoilsport may be the difference in efficiency when speed is increasing.

3.6.2. Type 2: assistance at the rear wheel

For two-wheelers of type 2, the control system determines assistance by measurements at the rear wheel. The assistance motor is mostly integrated in the rear wheel. The bicycle should be measured for all gears.

3.6.3. Averaging the signals

When applying a pulsating torque to the pedals, also speed and force are pulsating. For measuring ease, the displayed values are all averaged over 10 s. This equalled 100 measurement points for the used sampling frequency of 10Hz. (limited by the used multiplexer). By choosing the time-interval constant

(=10s), we make an averaging error depending on the rotational speed. The higher the pedal frequency is, the smaller the error when we do not have an integer number of pulses.

The pulsating character and thus the error will be most obvious in the torque signal. The frequency of the torque sine wave is twice the pedal frequency.

For the lowest measured pedal frequency (~2 rad/s=>0.31Hz) this results in a maximum error of 5% represented on figure 7. For the maximum pedal frequency (~2.5Hz) the maximum error is only 0.4%. This was considered to be sufficiently accurate for the first measurements.
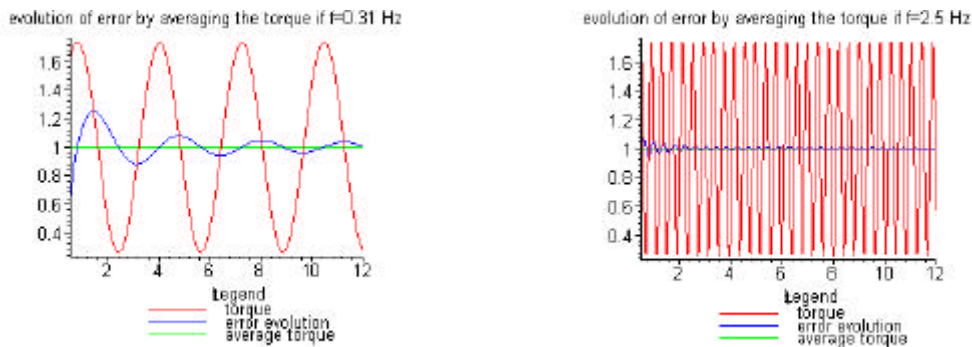
Figure 7: Evolution of the error by averaging the torque signal for f=0.31Hz and f=2.5Hz

4. Measurement Results

4.1. Type 1 Models

4.2. GMB Euro-scoot, L'avenir, (Merida), 2nd speed.

The merida is a type 1 EPAC. It was measured in 2nd speed. To check the statement in paragraph 3.6, we also took some measurements in the 4^{h} speed. A mean deviation of almost 10% of the expected values was observed. When the measurement method will be fully automated, it'll be recommended to also measure all speeds of the type 1 EPACs to include the impact of the transmission losses.

The difference in traction force between the case with and without assistance is displayed in fig. 8. Especially in figure 9, where the traction force is plotted versus the speed for fixed values of the real cyclist force, the doubling of the traction force is visible. This doubling diminishes slowly from 15 km/h and happens earlier for higher forces.
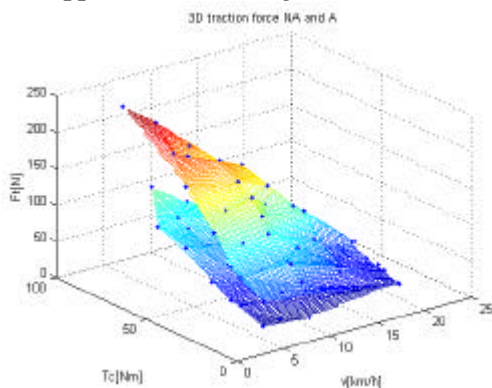
Figure 8: Output plot of the Merida in the 2nd speed
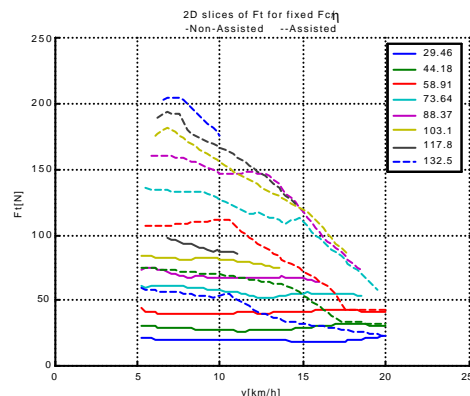
Figure 9: Slices of the performance plot of the Merida in the 2nd speed

Although the input was a pulsating torque, we'll use the simplified formulas to get the performance parameters. Comparison of the traction force for a pulsating input torque, and for a constant input torque with the same average, gave only a standard deviation of 3%.

From figures 10 and 11 it is clear that the efficiency of the (non-assisted) Merida is beneath the expected 95% of a ordinary bicycle. For the lower torques the efficiency even reduces to 60- 70%. Because of the simplified formulas, it concerns only a rough approximation of the efficiency. The low efficiency is a consequence of the extra transmission system for the motor torque
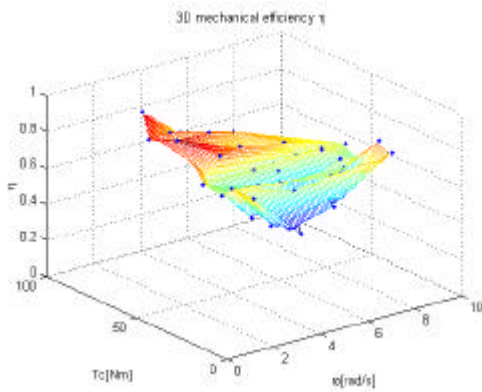
Figure 10: Efficiency plot of the Merida in the 2nd speed
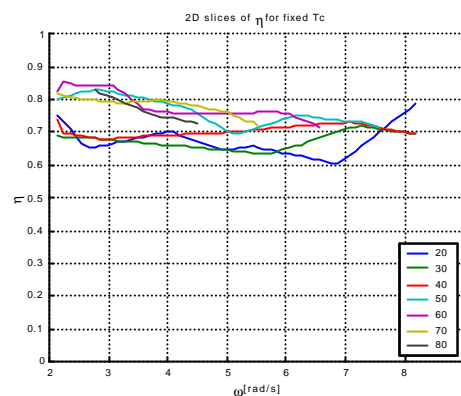
Figure 11: Evolution of the efficiency of the Merida as a function of rotational speed for different cyclist's torques

The assistance factor (for a definition, see 8) is shown in the figures 12 and 13. The assistance motor delivers 50% to 60% of the traction power in the area from 5 to 15 km/h. For the 2nd speed the assistance falls to zero at about 18 km/h. The specifications of the manufacturer mentions that assistance is given until 25 km/h. By using the transmission formula for the 4th speed, we get:

$$18.\frac{Z_4}{Z_2} = 18.\frac{0.985}{0.679} \approx 26km/h$$
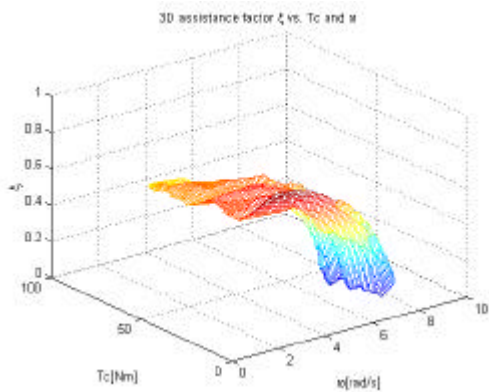
Figure 12: Evolution of the assistance factor of the Merida as a function of rotational speed and cyclist's torques
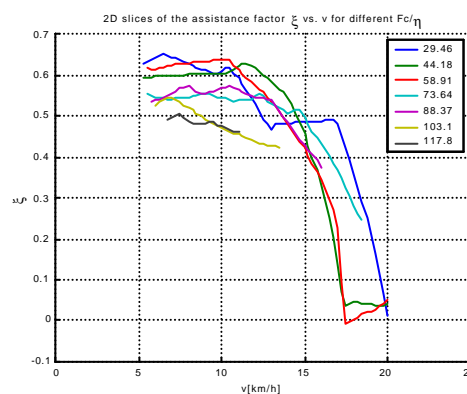
Figure 13: Evolution of the assistance factor of the Merida as a function of speed and cyclist's force

4.3. YamahaPAS, 2nd speed

Also the Yamaha is an EPAC of type 1 but it has an extra 'eco'-assistance mode. The traction force for 2nd speed was measured for several points of the operation area. Looking at figures 14 and 15 the eco-assistance seems to perfectly fit between the non-assisted and the fully assisted mode. In some case the assistance seems to triple the traction force.
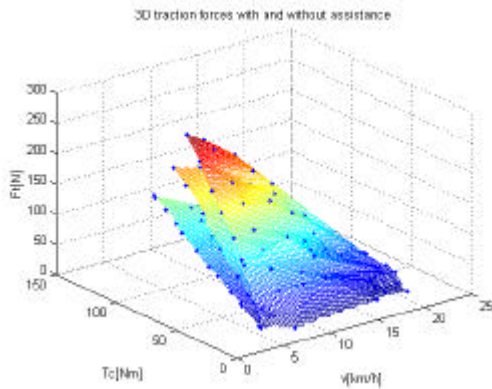

Figure 14: Output plot of the Yamaha PAS for 2nd speed in non-assisted, eco-assisted and assisted mode
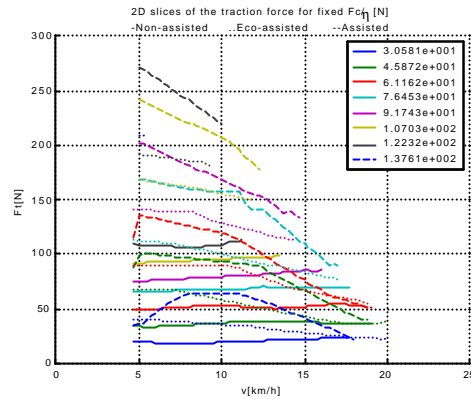
Figure 15: Slices of the performance plot of the Yamaha PAS for the three modes

About the performance parameters the same remarks can be given as for the Merida, although the efficiency seems to be a 10% higher. From figure 17 it is clear that especially for higher torques the assistance stays only slightly beneath the 60%, which is highly appreciated when driving the EPAC. A disadvantage of this high assistance power was felt during the test: we had to charge the battery twice for the pupose of the tests.
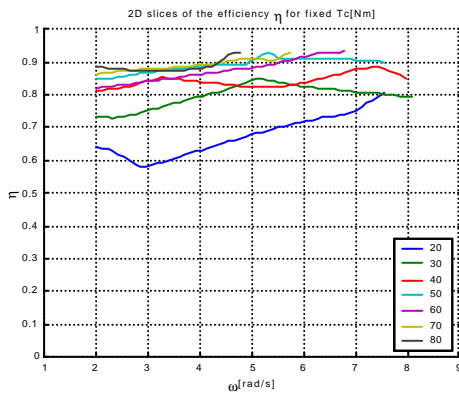

Figure 16: Evolution of the efficiency of the Yamaha PAS as a function of rotational speed for different cyclist's torques
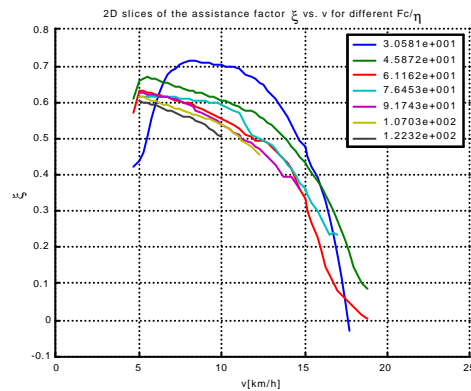
Figure 17: Evolution of the assistance factor of the Yamaha PAS as a function of speed and cyclist's force for the assisted mode

In eco-assistance the battery delivers only 30 to 45 % of the traction power (figure 18) resulting in a better life cycle of the battery. The speed at which the assistance diminishes seems to be equal in both assisted modes
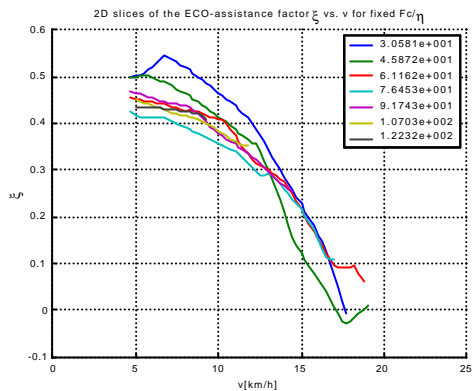
Figure 18: Evolution of the assistance factor of the Yamaha PAS as a function of speed and cyclist's force for the eco-assisted mode

4.4. Sachs elo-bike, 3rd speed
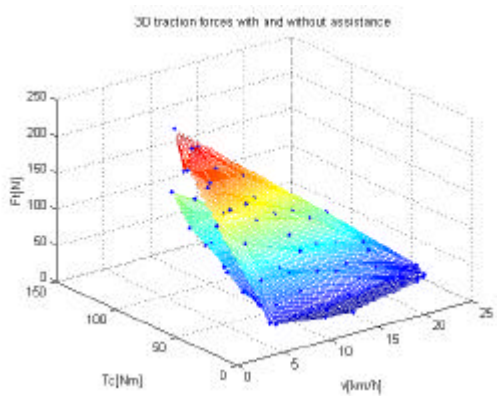
Figure 19: Output plot for the Sachs in 3rd speed with and without assistance.
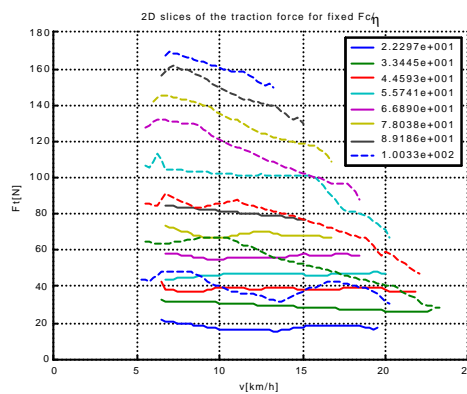
Fig. 20: Slices of the performance plot of the Sachs in 3rd speed with and without assistance.
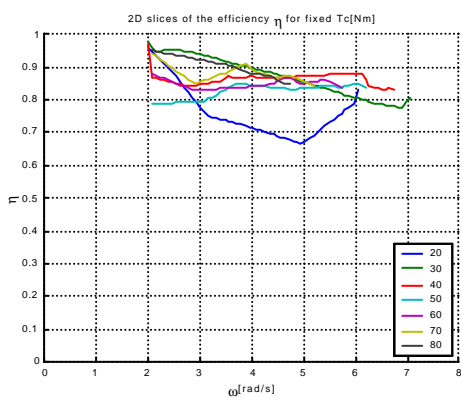
Fig. 21: Evolution of the efficiency of the Sachs as a function of rotational speed for different cyclist's torques.
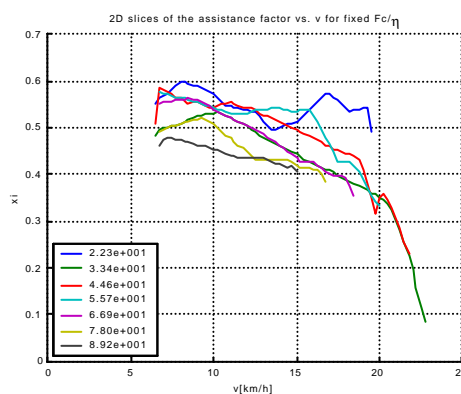

Fig. 22: The assistance factor of the Sachs in 3rd speed as function of speed for different cyclist's forces.

The Sachs elo-bike is an EPAC of type 2, so measurements have been taken in all 3 speeds. The traction forces for different speeds were related to each other as were the transmission factors Z.

So the control system of the assistance motor seems to measure the cyclist's torque behind the gear. It suffices to give one speed to get an idea of the performance of this EPAC.

In figures 19 and 20 the results of the 3rd speed measurements of the Sachs are given.

The performance parameters η and ξ are presented in figures 21 and 22. The efficiency lies between 80 and 90%. Remarkable is the smoother evolution of ξ for higher torques. The assistance motor effect stops at about 22 km/h.

5. Conclusions

The measurements on the test bench confirm and quantify the driving comfort experienced on the electric bicycles YamahaPAS, Merida Pre-Scoot and Sachs elo-bike. The consequence of the assistance factor for the range of the bicycles has to be further investigated.

The mechanical efficiency of the 3 tested EPACs, measured with assistance switched off, is significantly lower than of a normal bicycle. This makes the EPACs hard to drive when the assistance drops down.

The electric assistance factor is only constant over a small speed area, diminishes slightly for higher speeds and drops down at a rotational speed of typically 7 rad/s (~25km/h in highest speed) for Merida and YamahaPAS and at 22 km/h for the Sachs elo-bike.

These first tests enabled us to optimise the test bench, the data acquisition system and the calculation and visualisation of the performance parameters of EPACs. Further adaptations in the data acquisition system have to be made to optimise the calculation of the traction power for pulsating input torques. Other EPACs will be tested and the performance parameters will be compared to the impression fed back by the users. This will be reported in later publications.

6. References

[1]   D. Goethals, N. Smets, *Test bench for EPACs*, final report VUB, 2002

[2]   P. Van den Bossche, V. Gallet, *user needs study*, E-tourproject WP2-1, 2002

[3]   A. W. Jackson, M. Dragovan, *An experimental investigation of bicycle dynamics*, Cycling Resources, http://www.bsn.com/cycling/articles/

[4]   Jones, David E. H., *The stability of the bicycle*, Physics Today, April 1970, 34-40

[5]   Philippe Lataire et al., Electrically assisted bicycles demonstration in Brussels, EVS-18, Berlin October 2001, paper PP289

7. Affiliation

Ir. Jan Cappelle
Kaho Sint-Lieven, Gebr. Desmetstraat 1, B-9000 Gent
VUB University of Brussels
Tel: +32 9 324 68 35   Fax:+32-9-265 86 25   E-mail:jan.cappelle@kahosl.be

Vita: Jan Cappelle is affiliated as PhD student at the university of Brussels. He gives lectures in elektrotechnics at the KaHo Sint-Lieven industrial engineering school in Ghent.

Prof. Dr. Ir. Philippe Lataire, Vrije Universiteit Brussel
Prof.Gaston Maggetto, Vrije Universiteit Brussel
Prof. Dr. Romain Meeusen, Vrije Universiteit Brussel
Mr. Farid Kempenaers, Vrije Universiteit Brussel